Supplementary Information

Effect of Si content on structure and electrochemical performance of ternary nanohybrids integrating Si nanoparticles, N-doped carbon shell, and nitrogen-doped graphene

Dehui Ji [a], Zhiwei Yang [a], Lingling Xiong [a], Honglin Luo [a,b,*], Guangyao Xiong [a], Yong Zhu [c], Yizao Wan [a,b,*]

[a] *School of Materials Science and Engineering, East China Jiaotong University, Nanchang 330013, China*

[b] *School of Materials Science and Engineering, Tianjin University, Tianjin 300072, China*

[c] *School of Chemical Engineering, Tianjin University, Tianjin 300072, China*

Corresponding authors.

Honglin Luo:

E-mail address: hlluotju@126.com; Tel: +86 22 2740 3045; Fax: +86 22 2740 4724

Yizao Wan:

E-mail address: yzwantju@163.com; Fax & Tel: +86 791 8704 6425

Experimental

In a typical procedure, varying amount (setting the ratio of Si : glucosamine hydrochloride : graphene oxide (GO) at 1 : 2 : 1, 2 : 2 : 1, 4 : 2 : 1, and 6 : 2 : 1) of Si powder (~80 nm, Alfa Aesar) was dispersed in deionized water by sonication for 2 h, followed by addition of aqueous solution containing glucosamine hydrochloride (≥99 %, Sigma-Aldrich) under stirring. Afterwards, GO aqueous dispersion (2 mg mL^{-1}, Institute of Coal Chemistry, Chinese Academy of Science) was added and the mixture was subjected to sonication to obtain a fully homogeneous solution. The water in the mixed solution was evaporated at 100 °C under vigorous stirring to obtain a seriflux, which was freeze-dried overnight. The resultant product was heated to 800 °C in a tube furnace and kept at that temperature under flowing argon for 2 h, resulting in four hybrids of Si/NC/NG-1, Si/NC/NG-2, Si/NC/NG-3, and Si/NC/NG-4, respectively, corresponding to the aforementioned ratios.

X-ray diffraction (XRD) data were collected on a Bruker D8 Advanced XRD Diffractometer using Cu Kα radiation (λ = 1.54056 Å, 40 kV, 40 mA). A field emission scanning electron microscope (SEM, FEI Nanosem 430) was used to observe the morphology of various samples. Transmission electron microscopy (TEM) and high-resolution TEM (HRTEM) analyses were carried out using a JEOL JEM-2100F microscope. Raman spectra were obtained using a DXR Raman microscope with a 532 nm laser excitation. X-ray photoelectron spectroscopy (XPS) analysis was carried out using a PHI1600 ESCA system with Al Kα X-ray radiation as the source for excitation. The elemental compositions were obtained from an element analyzer (EA, Vario EL). Thermogravimetric analysis (TGA) was carried out with a heating rate of 10 °C min^{-1} in air up to 800 °C using a Netzsch STA 449C thermal analyzer. For the preparation of working electrodes, a mixture of active material, carbon black,

and polyvinylidene difluoride (PVDF) binder in a weight ratio of 80 : 10 : 10 was prepared with N-methylpyrrolidone (NMP) as the solvent. The resultant homogeneous slurry was uniformly coated on the surface of copper foil (used as a current collector) and dried at 100 °C under vacuum overnight. Coin-type cells were assembled in an Ar-filled glove box using a separator (Celgard 2400), a counter electrode made of Li metal foil, and an electrolyte of 1.0 M $LiPF_6$ in a mixture of ethylene carbonate (EC), dimethyl carbonate (DMC), and diethyl carbonate (DEC) at a volume ratio of 1 : 1 : 1. Each half-cell was aged for 24 h after assembly. Charge-discharge experiments were performed at a constant current density between 0.01 and 1.5 V (*vs*. Li^+/Li) using a BTS-5V10mA battery tester at room temperature. The galvanostatic cycling tests were carried out on a battery testing system (Neware Electronic Co., China) in the potential range of 0.01-1.5 V at room temperature. Electrochemical impedance spectroscopy (EIS) tests were performed on a CHI660D electrochemical workstation over a frequency range of 0.1 MHz - 0.01 Hz at an AC amplitude of 5 mV.

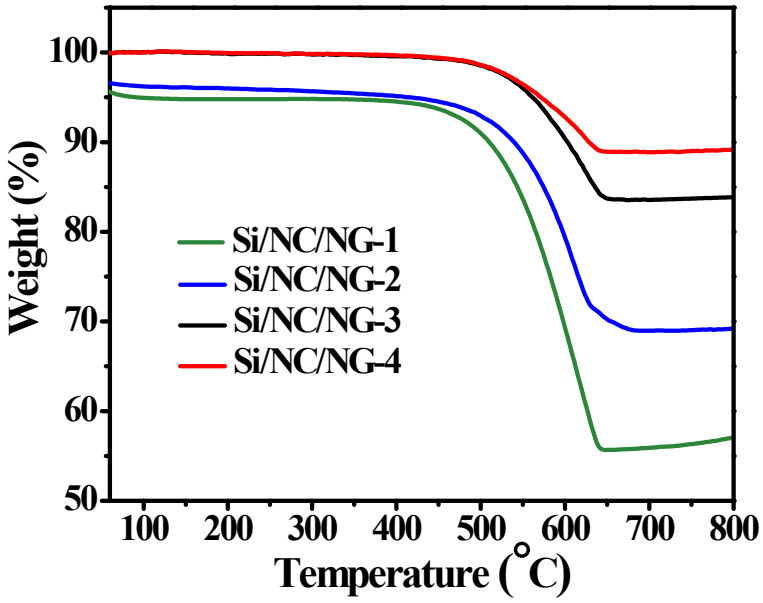

Figure S1. TGA curves of Si/NC/NG nanohybrids with varying Si contents.

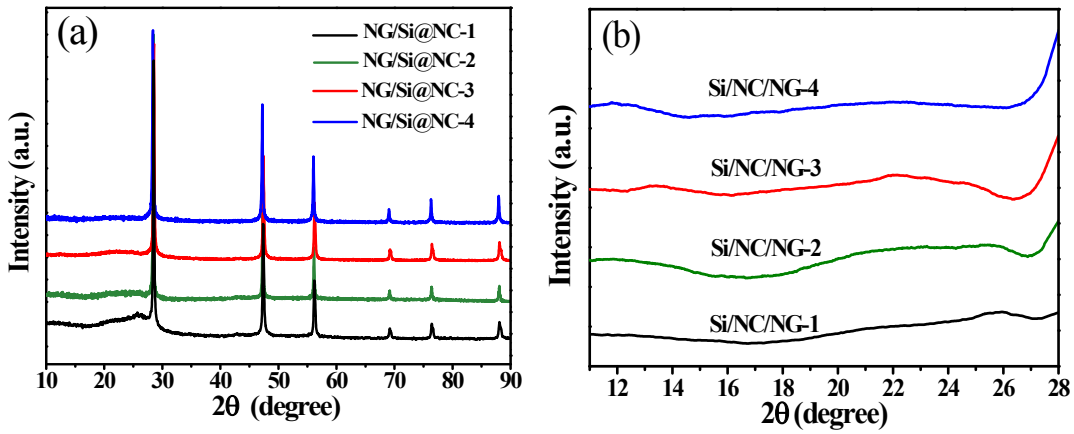

Figure S2. XRD patterns of Si/NC/NG nanohybrids with varying Si content (a) and the magnified portion from 11 to 28 degree (b).

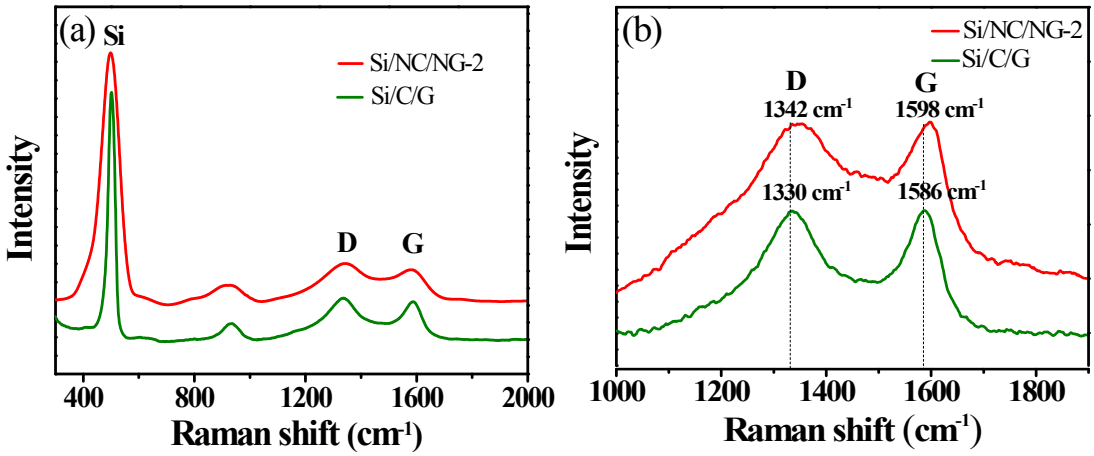

Figure S3. Raman spectra of Si/NC/NG and Si/C/G (a) and the magnified portion of D and G bands (b)..

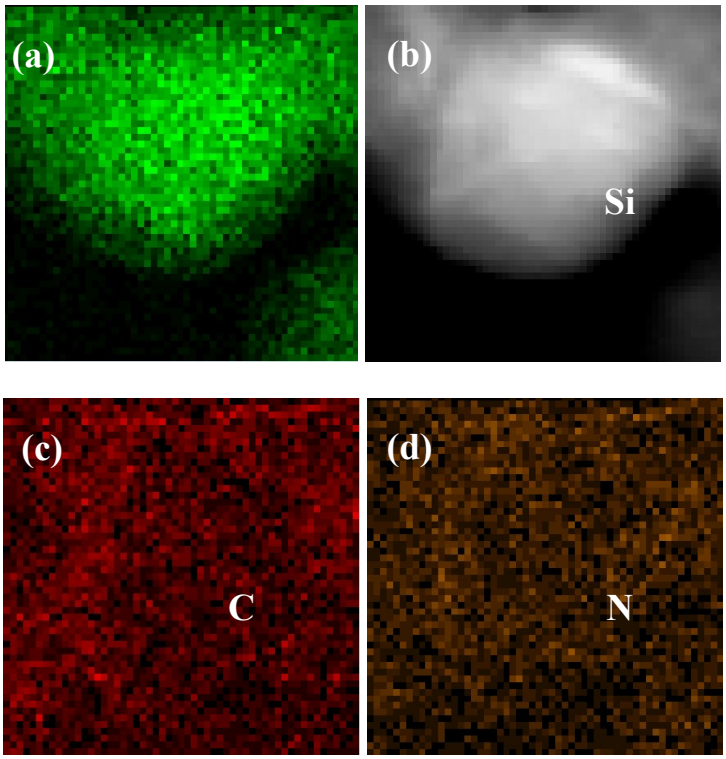

Figure S4. (a) SEM image of the selected NG-enwrapped Si/NC nanoparticle for EDS mapping, (b), (c), and (d) are Si, C, N elemental distributions, respectively.

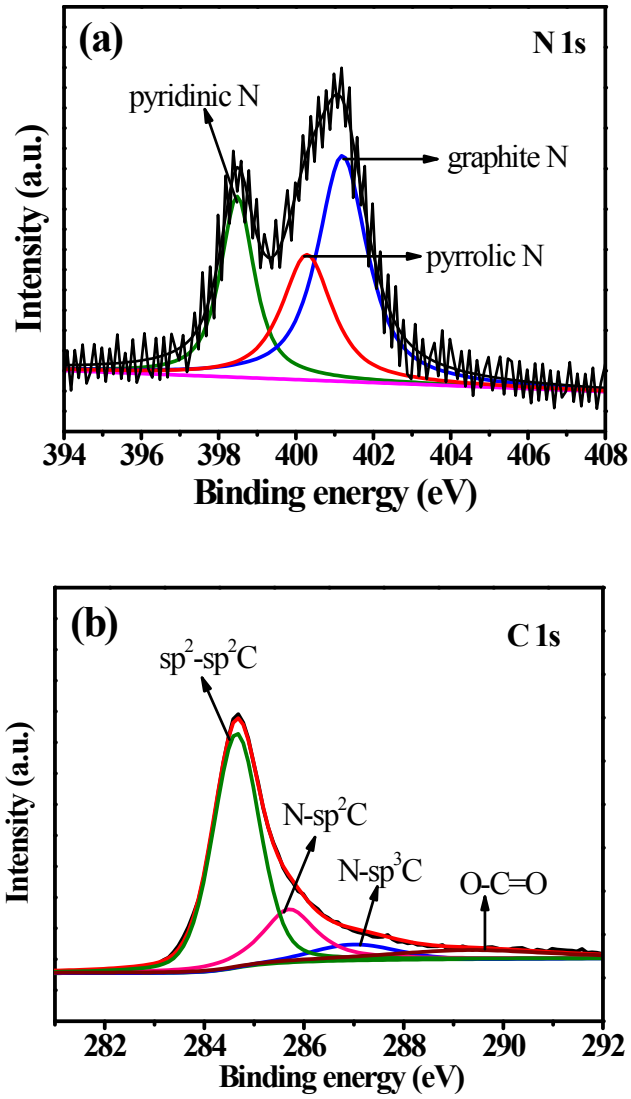

Figure S5. XPS spectra of N1s (a) and C1s (b). As shown in Fig. S5a, the spectrum of N element can be deconvoluted into three sub-peaks located at 398.4, 399.8, and 401.1 eV corresponding to pyridinic N (49.7 wt%), pyrrolic N (32.3 wt%), and graphitic N (18.0 wt%), respectively [1, 2] with a total N-doping level of around 4.2 wt%. The N-doping is believed to cause stronger interaction between the formed carbon structure and lithium owing to the higher electronegativity of nitrogen (3.5) than carbon (3.0) and its smaller diameter than carbon. The N-doping also generates defects in the graphite structure and improve the interfacial interaction, thus enhancing the reversible capacity [3-7]. Fig. S5b shows the C 1s peak ranging from 281-292 eV, which can be split into four sub-peaks, located at 284.6, 289.3, 285.7, and

287.0 eV, corresponding to C-C, C=O, C-N, and C=N, respectively [6, 8, 9]. The presence of C-N and C=N is due to substitution of the N atoms and defects or the edge of the NG and/or carbon [6, 8],

References

1. D. Wei, Y. Liu, Y. Wang, H. Zhang, L. Huang and G. Yu, *Nano Lett* 2009, **9**, 1752-1758.

2. Y. J. Cho, H. S. Kim, H. Im, Y. Myung, G. B. Jung, C. W. Lee, J. Park, M.-H. Park, J. Cho and H. S. Kang, *J Phys Chem C* 2011, **115**, 9451-9457.

3. Y. J. Cho, H. S. Kim, H. Im, Y. Myung, G. B. Jung, C. W. Lee, J. Park, M.-H. Park, J. Cho and H. S. Kang, *The Journal of Physical Chemistry C* 2011, **115**, 9451-9457.

4. H. Ming, J. Ming, X. Li, Q. Zhou, L. Jin, Y. Fu, J. Adkins, Z. Kang and J. Zheng, *RSC Adv* 2013, **3**, 15613.

5. Z. Ding, L. Zhao, L. Suo, Y. Jiao, S. Meng, Y. S. Hu, Z. Wang and L. Chen, *Physical chemistry chemical physics : PCCP* 2011, **13**, 15127-15133.

6. H. Wang, C. Zhang, Z. Liu, L. Wang, P. Han, H. Xu, K. Zhang, S. Dong, J. Yao and G. Cui, *J Mater Chem* 2011, **21**, 5430-5434.

7. Y. Li, J. Dong, J. Zhang, X. Zhao, P. Yu, L. Jin and Q. Zhang, *Small* 2015, **11**, 3476–3484.

8. L. Wang, Y. Zheng, X. Wang, S. Chen, F. Xu, L. Zuo, J. Wu, L. Sun, Z. Li, H. Hou and Y. Song, *ACS applied materials & interfaces* 2014, **6**, 7117-7125.

9. M. Bou, J. M. Martin, T. Le Mogne and L. Vovelle, *Appl Surf Sci* 1991, **47**, 149-161.